Vol. 46, No. 2 (2024) 332-345, DOI: 10.24874/ti.1598.12.23.04

Tribology in Industry

www.tribology.rs

RESEARCH

Method for a Comprehensive Analytical Study of Contact Pressures, Wear, and Durability of Metal-Polymer Helical and Spur Gears with Steel Pinion and Polyamide Gear

Myron Czerniec[a,*], Marek Opielak[b], Jerzy Czerniec[c]

[a]*National Aviation University, 1, Liubomyra Huzara ave., Kyiv, 03058, Ukraine,*
[b]*Technical University of Lublin, Nadbystrzycka Street 36, Lublin, 20-618, Poland,*
[c]*Lublin Academy WSEI, 4 Projektowa str., Lublin, 20-209, Poland,*
[d]*National Aviation University, 1, Liubomyra Huzara ave., Kyiv, 03058, Ukraine.*

Keywords:

Metal-polymer gears
Polyamides
New author's analytical method
Contact pressures
Wear
Durability

* Corresponding author:

Myron Czerniec
E-mail: myron.czerniec@gmail.com

Received: 27 December 2023
Revised: 26 February 2024
Accepted: 25 April 2024

A B S T R A C T

An analytical complex study of metal-polymer (MP) helical and spur gears by a new author's analytical method was carried out. The influence of the helix angle on the contact pressures in the engagement, the teeth wear, and the durability of the MP gears of different polymers has been established. MP gears with a pinion made of carbon steel (0.45% C) and gear made of basic polyamides PA6, PA66, and their composites with the following fillers: fiberglass (PA6+30GF), carbon fiber (PA6+30CF), molybdenum disulfide (PA6+MoS_2), and oil filled cast polyamide (PA6+Oil) are studied. According to the developed procedure for determination of the angles of engagement parity change, it is shown that there is two-one-two-pair or three-two-three-pair engagement depending on the helix angle. Quantitative and qualitative regularities of changes in the initial maximum contact pressures and their reduction due to tooth wear over the time from the moment of the entrance of teeth to engagement up to their exit from it are established. In particular, at a helix angle of β = 10°, the contact pressures reduce to 33% compared to spur gears. The linear wear of the gear polymer tooth profile h_{2j} at selected points of engagement and different helix angles has been investigated, and the influence of the pressure angle on it is shown. It is established that its regularities of change during the engagement phase are the same for all polymeric materials studied. The durability of transmissions is calculated, and its comparative evaluation is given. At the helix angle β = 5°, a slight increase in durability is achieved compared to spur gears, and at β = 10° the durability of MP gears increases by about 1.5 times for all polymeric materials studied.

1. INTRODUCTION

The use of polymeric materials in metal-polymer (MP) gears operating in friction conditions without lubrication is quite common, in particular polyamides both unreinforced (PA6, PA66) and composites with different fillers (glass and carbon fiber, molybdenum disulfide, graphite, carbonite, bronze powder, polyethylene, PTFE, oil, etc.) and different volume content. It is known that in such a way it is possible to improve their mechanical properties, especially wear resistance. Accordingly, the durability of MP gears will also increase. Common polymeric materials for MP gears are polyamide PA6 and its composites PA6+30GF, PA6+30CF, PA6+MoS_2, and PA6+Oil, thanks to their good mechanical, technological, operational, and tribological properties.

An urgent task of triboengineering is to meet the challenges of engineering practice with the development of computational and numerical methods for research of MP and polymer gears for their contact strength, wear resistance, and durability. However, despite the urgency of solving this important for science and engineering problem in connection with the growing use of these types of polymer gears, effective calculation methods for assessing their performance have not yet been developed. Previously, in using a simplified calculation method [2] based on Archard's law of abrasive wear, a partial study of MP spur gears with a gear made of PA6+30GF, PA6+30CF with dispersed fibers has been conducted [1]. As for studies of MP gears by different numerical methods for their wear resistance and durability, they have not yet been carried out.

In [3], the behavior of a number of polymers and polymer composites was studied. Acetal PA6 was the best of the unreinforced polymers. The wear of the studied materials was significantly differentiated. In some works [4,5], there are results of calculation of contact and bending tooth strength of MP spur gears. The influence of the load distribution among the gears on the specified stresses in the MP gears with a PA66 polyamide gear paired with a steel pinion has been established in [4]. And in [5], the maximum contact pressures of the same gears have been estimated.

The previous tribological studies of polymeric materials for gears have yielded different results. In particular, experimental studies of the volumetric tooth wear of model MP gears were conducted in [6-8]. Gears made of PA6-Mg, PA6-Na, PA66+30GF paired with S355 steel in the presence of abrasive and without it were studied in [6,7]. The wear of gears made of PA6 was studied in [8] for various types of MP gears (spur, bevel, and worm).

The tribological behavior of different types of polyamides for MP gears paired with steel has been studied on a pin-on-disk testing machine. In particular, work [9] is devoted to the wear resistance of the tribocouple PA66 - steel SAE 1045, used in clutch discs. Also, in [10-12] the tribological behavior of PA6 polyamide during dry friction was studied under different operation conditions.

A number of works are devoted to the experimental study of polymer gear wear, in particular, gears made of polyamides and their composites [13-19]. In [13], the tribological behavior of wheels made of PA6, PA66, PA46, and PA12, reinforced with carbon fiber was studied. Accelerated tests of polymer gears [14] were performed on 15 different compositions filled with glass or carbon fiber and unfilled PA6, PA66, and POM. A detailed study on the friction and wear of gears made of acetal POM and PA6 in the same type and mixed pairs was described in [15]. PA6 filled with fiberglass and Teflon was studied in [16]. The work [17] is devoted to the wear of 27 pairs of gears made of PA66, PA66+15GF, and PA66+30GF. In [18], the wear resistance of polymer gears made of PA66, polyester PEEK, and POM at different loads and speeds has been investigated. The work [19] contains the results of testing the wear of gears made of PA filled with 30% glass or 25% SiC, PA6 with 25% SiC, and PA66 with 25% SiC.

However, the results of the wear resistance studies of polymeric materials on tribo-testers according to the pin-on-disk scheme or other standardized schemes of sliding friction, as well as on model gears are difficult to use when calculating gears for durability. The main reason for such difficulty is conducting research at one value of load (tribotesting machine) or one torque (model gears), and thus the obtained Archard's coefficient of abrasion cannot be used at other loads.

Therefore, an urgent scientific and engineering problem is the development of effective methods for estimating the wear and service life of gears made of polymer composite materials, which take into account the results of representative model tribo-experimental studies in modeling the kinetics of wear. Accordingly, in [20-24] the author's method of MP gears calculation based on the phenomenological methodology of wear resistance research of materials at sliding friction [20,25-28] by frictional-fatigue wear mechanism is given. This approach is fundamentally different from the current approach to the mechanism of wear of metal-polymer and polymer tribocouples, which adopts Archard's law for adhesive-abrasive wear.

It should be noted that statistical data on the causes of the functional capacity loss of various tribomechanical systems indicate that the main reason in 85 - 95% of cases is the wear of their elements, which is generally known. The teeth failures of MP gears operating under dry friction conditions, such as breakage near the root, chipping at the edge, increased plastic deformation or local fatigue failure (pitting) occur much less often and are usually caused by non-compliance with the loading or temperature regime of operation.

The aim of this work is to mathematically model the contact and tribocontact interaction in the meshing of a metal-polymer spur gear. According to the developed new generalized author's method, the article studies the contact strength (load carrying capacity), wear, and service life of helical and spur gears with a gear made of polyamides PA6, PA66, and composites PA6+30GF, PA6+30CF, PA6+MoS_2, and PA6+Oil. Changes in contact parameters due to tooth wear and changes in their parity of engagement. There have been described no methods in the literature to solve the problem of studying MP gears in such a statement.

2. METHOD FOR STUDY OF WEAR AND DURABILITY OF HELICAL AND SPUR GEARS

The general view of MP gears is given in Fig. 1.

(a)

(b)

Fig. 1. Metal-polymer gears: (a) helical, (b) spur.

When calculating helical gears, the following characteristics should be determined:

- initial maximum contact pressures $p_{j\max}$ at any *j*-th point of the tooth profile;
- maximum contact pressure $p_{jh\max}$ due to tooth wear;
- gear polymer tooth linear wear h_{2j} at any *j*-th point of the profile;
- minimum gears durability t_{min}.

2.1. Function of linear wear of teeth

With taking into account the peculiarities of teeth' contact during their interaction, the function of their linear wear h'_{kj} can be expressed by the formula (1). This formula is used for calculation of helical gears at any *j*-th point of tooth profile over a single time t'_j of tribocontact in a one-pair engagement [23-26,28]:

$$h'_{kj} = \frac{v_j t'_j \left(f p_{j\max} \right)^{m_k}}{C_k \left(0.5 R_m \right)^{m_k}} = \frac{v_j t'_j \left(\tau_{j\max} \right)^{m_k}}{C_k \left(\tau_S \right)^{m_k}}, \quad (1)$$

where $t'_j = 2b_j / v_0 =$ var; $v_0 = \omega_1 r_1 \sin \alpha_t$; $\tau_{j\max} = f p_{j\max}$.

2.2. Contact parameters

The initial maximum contact pressures $p_{j\max}$ and the contact area width $2b_j$ at the *j*-th point of the profile are calculated by Hertz's formulas

$$p_{j\max} = 0{,}564\sqrt{N'/\theta\rho_j}\,,$$
$$2b_j = 2{,}256\sqrt{\theta N'\rho_j}\,, \qquad (2)$$

where $N' = N/l_{\min}w$; $N = T_{nom}K_g / r_1\cos\alpha_t$; $T_{nom} = 9550P/n_1$; $\theta = \left(1-\mu_1^2\right)/E_1 + \left(1-\mu_2^2\right)/E_2$.

The initial radii of curvature of tooth profiles at the *j*-th point of helical gear (reduced radius ρ_j, for a pinion ρ_{1j}, for a gear ρ_{2j})

$$\rho_j = \frac{\rho_{1j}\rho_{2j}}{\rho_{1j}+\rho_{2j}},\ \rho_{1j} = \frac{\rho_{t1j}}{\cos\beta_b},\ \rho_{2j} = \frac{\rho_{t2j}}{\cos\beta_b}, \qquad (3)$$

where

$\beta_b = \arctan\left(\tan\beta\cos\alpha_t\right)$, $\alpha_t = \arctan\left(\dfrac{\tan\alpha}{\cos\beta}\right)$,

$\rho_{t1j} = r_{b1}\tan\alpha_{t1j}$, $\rho_{t2j} = r_2\sqrt{\left(r_{2j}/r_2\right)^2 - \cos^2\alpha_t}$,

$\alpha_{t1j} = \arctan\left(\tan\alpha_{t10} + j\Delta\varphi\right)$,

$\alpha_{t2j} = \arccos\left[\left(r_2/r_{2j}\right)\cos\alpha\right]$, $r_{b1} = r_1\cos\alpha_t$,

$r_{b2} = r_2\cos\alpha_t$, $r_1 = mz_1/2\cos\beta$,

$\tan\alpha_{t10} = \left(1+u\right)\tan\alpha_t - \dfrac{u}{\cos\alpha_t}\sqrt{\left(r_{20}/r_2\right)^2 - \cos^2\alpha_t}$,

$r_{20} = r_{a2} - r$, $r_{a2} = r_2 + m$,

$r_{2j} = \sqrt{a^2 + r_{1j}^2 - 2ar_{1j}\cos\left(\alpha_t - \alpha_{t1j}\right)}$,

$r_{1j} = r_1\cos\alpha_t/\cos\alpha_{t1j}$, $a = \left(z_1+z_2\right)m/2\cos\beta$,

$\tan\alpha_{t1s} = \arctan\sqrt{\left(r_{1s}/r_1\right)^2 - \cos^2\alpha_t}$, $r_{1s} = r_{a1} - r$,

$r_{a1} = r_1 + m$,

$\tan\alpha_{t2s} = \left(1+u^{-1}\right)\tan\alpha_t -$
$- \dfrac{1}{u\cos\alpha_t}\sqrt{\left(r_{1s}/r_1\right)^2 - \cos^2\alpha_t}$.

The minimum length of the contact line

$$l_{\min} = \frac{b\ \varepsilon_\alpha}{\cos\beta_b}\left[1 - \frac{\left(1-n_\alpha\right)\left(1-n_\beta\right)}{\varepsilon_\alpha\varepsilon_\beta}\right] \text{ at } n_\alpha + n_\beta > 1,$$

$$l_{\min} = \frac{b\ \varepsilon_\alpha}{\cos\beta_b}\left[1 - \frac{n_\alpha n_\beta}{\varepsilon_\alpha\varepsilon_\beta}\right] \text{ at } n_\alpha + n_\beta \le 1, \qquad (4)$$

where $\varepsilon_\alpha = \dfrac{z_1(e_1+e_2)}{2\pi r_{b1}}$, $\varepsilon_\beta = \dfrac{b\ \sin\beta}{\pi m}$,

$e_1 = \sqrt{r_{1s}^2 - r_{b1}^2} - r_1\sin\alpha_t$, $e_2 = \sqrt{r_{20}^2 - r_{b2}^2} - r_2\sin\alpha_t$.

Contact parameters such as the contact wear pressures $p_{jh\max}$ and the tribocontact width $2b_{jh}$ are calculated considering the tooth wear according to the modified Hertz formulas

$$p_{jh\max} = 0{,}564\sqrt{N'/\theta\rho_{jh}}\,,$$
$$2b_{jh} = 2{,}256\sqrt{\theta N'\rho_{jh}}\,, \qquad (5)$$

where $\rho_{jh} = \dfrac{\rho_{1jh}\rho_{2jh}}{\rho_{1jh}+\rho_{2jh}}$.

The variable radii of curvature ρ_{kjh} are calculated by our method described in [22,26-28].

2.3. Sliding speed in engagement

The sliding speed is calculated as follows

$$v_j = \omega_1 r_{b1}\left(tg\alpha_{t1j} - tg\alpha_{t2j}\right). \qquad (6)$$

2.4. Changing the parity of teeth

The angle $\Delta\varphi_{1F_2}$ of the tooth entrance to the one-pair engagement and the angle $\Delta\varphi_{1F_1}$ of the exit from it are determined by the relations:

$$\Delta\varphi_{1F_2} = \varphi_{10} - \varphi_{1F_2},\ \Delta\varphi_{1F_1} = \varphi_{10} + \varphi_{1F_1}, \qquad (7)$$

where

$\varphi_{1F_2} = \tan\alpha_{F_2} - \tan\alpha_t$, $\varphi_{1F_1} = \tan\alpha_{F_1} - \tan\alpha_t$,

$\varphi_{10} = \tan\alpha_{t10} - \tan\alpha_t$, $p_b = \pi m\cos\alpha_t/\cos\beta$;

$$\tan\alpha_{F_2} = \frac{r_1\sin\alpha_t - (p_b - e_1) + 0.5p_b n_\beta}{r_1\cos\alpha},$$

$$\tan\alpha_{F_1} = \frac{r_1\sin\alpha_t - (p_b - e_2) - 0.5p_b n_\beta}{r_1\cos\alpha}. \qquad (8)$$

The angle $\Delta\varphi_{1E}$ of the tooth exit from the engagement

$$\Delta\varphi_{1E} = \varphi_{10} + \varphi_{1E}, \qquad (9)$$

where $\varphi_{1E} = \tan\alpha_E - \tan\alpha_t$, $\alpha_E = \arccos(r_{b1}/r_{1s})$.

In the case of three-two-three-pair tooth engagement, when $2 \le \varepsilon_\gamma = \varepsilon_\alpha + \varepsilon_\beta < 3$, relations (8) can be used only if the fractional parts n_α, n_β of the coefficients $\varepsilon_\alpha, \varepsilon_\beta$ of the end and pitch overlap correspond to the relation $n_\alpha + n_\beta < 1$. If $n_\alpha + n_\beta \ge 1$, they do not yield the correct values of angles $\Delta\varphi_{1F2}$ and $\Delta\varphi_{1F1}$. Then the following expressions to determine $\tan\alpha_{F_2}$ and $\tan\alpha_{F_1}$ should be used:

$$\tan\alpha_{F_2} = \frac{r_1 \sin\alpha_t - (p_b - e_1) + 0.5 p_b (1 - \varepsilon_\beta)}{r_1 \cos\alpha}$$
$$\tan\alpha_{F_1} = \frac{r_1 \sin\alpha_t - (p_b - e_2) - 0.5 p_b (1 - \varepsilon_\beta)}{r_1 \cos\alpha} \qquad (10)$$

2.5. Durability of gears

To solve the problem of durability of gears, our before-developed block scheme of calculation [22-26,28] was used. For the number of revolutions of the pinion n_{1s} and the gear n_{2s}, which corresponds to the number of interaction blocks B of the accepted size under constant contact conditions, the total tooth wears h_{1jn} and h_{2jn} at the j-th points of contact are determined as follows:

$$h_{1jn} = \sum_{1}^{n_{1s}} h_{1jB}\,, \quad h_{2jn} = \sum_{1}^{n_{2s}} h_{2jB} \qquad (11)$$

where $n_{2s} = n_{1s} / u$; $h_{kjB} = \sum h'_{kj}$ is the tooth wear in each block of interaction.

When the initial contact pressures $p_{j\max}$ change because of tooth wear, the duration of the gear operation t_B at the number of revolutions n_{1s} or n_{2s} of toothed wheels is calculated as follows:

$$t_B = n_{1s} / 60 n_1 = n_{2s} / 60 n_2\,. \qquad (12)$$

3. NUMERICAL SOLUTION AND DISCUSSION

Involute helical and spur MP gears with steel pinions and polymer gears were studied.

Initial data

T_{nom} = 4000 Nmm, n_1 = 700 rpm; B = 420,000 rev (10 hours of operation); K_g = 1.2; m = 4 mm, u = 3, z_1 = 20, z_2 = 60, b = 50 mm, β = 0°, 5°, 10°, h_{2*} = 0.5 mm.

Materials

Pinion: carbon steel 0.45% C, normalization, grinding, E_1 = 2.1·10^5 MPa, μ_1= 0.3; C_1 = 10^9, m_1= 2; τ_{S1}= 345 MPa.

Gear: polyamides (PA) and composites based on them (Table 1).

Table 1. Characteristics of polyamides and composites used.

Characteristics	Thermoplastic polymeric materials					
	PA6 (Sustamid 6 Rochling)	PA66 (Sustamid 66 Rochling)	PA6+ 30GF (Sustamid 6 GF30 Rochling)	PA6+ MoS_2 (Sustamid 6 MO Rochling)	PA6+30CF (Sustamid 6 ESD 60 Rochling)	PA6+ Oil (Sustamid 6 OL Rochling)
Young's modulus E_2, MPa	2000	2300	2700	1660	3300	1960
Poisson's ratio μ_2	0.4	0.4	0,41	0,4	0,41	0,4
Friction coefficient f	0.23	0.23	0.31	0.23	0.25	0.25

Note: PA6+30GF – fiberglass filler (30 vol% of fine fibers), PA6+30CF – carbon fiber (30 vol% of fine fibers), PA6+MoS_2 – molybdenum disulfide, PA6+Oil – oil-filled cast polyamide.

The coefficient of friction was determined by experimental studies of the tribological behavior of metal-polymer pairs in dry friction using the pin-on-disk scheme according to the method [20]. Also, as a result of these model studies of the wear resistance of polymeric materials, their wear resistance characteristics C_2, m_2 are given in Table 2.

Table 2. Polyamides and composites based on them.

Wear resistance characteristics	**Thermoplastic polymeric materials**					
	PA6	PA66	PA6+ 30GF	PA6+ MoS_2	PA6+ 30CF	PA6+ Oil
Linear wear resistance characteristic of gear material, $C_2 \cdot 10^6$	1.34	1.98	1.88	3.08	3.67	4.20
Power law wear resistance characteristic of gear material, m_2	1.15	1.15	1.15	1.15	1.15	1.15
Shear strength τ_S , MPa	40	40	50	38	40	38

Note: the characteristics C, m are established by the pin-on-disk scheme under dry friction at T = 23±1°C and relative humidity of 50 ± 5% (ISO 7148-2 standard [29]).

The results of studies for the influence of the helix angle on the maximum initial contact pressure and pressure after wear, the linear wear of tooth profiles, and gear durability are shown in Figs. 2 – 7. Figures 2-4 demonstrate the change in the initial maximum contact pressures $p_{j\max}$ in the cycle of two-one-two-pair engagement $(\beta = 0°,\ 5°)$ (Figs. 2a and 3a) and three-two-three-pair engagement $(\beta = 10°)$ (Fig. 4a). Accordingly, Fig. 2b, 3b, and 4b show contact pressures $p_{jh\max}$ after wear when reaching the acceptable gear tooth wear h_{2*} = 0.5 mm at one of the points of engagement.

The figures on the left show the area of the left phase of two-pair $(\beta = 0°,\ 5°)$ or three-pair $(\beta = 10°)$ engagement. The area changes with increasing the helix angle. In the case of two-one-two-pair engagement (Fig. 2a and 3a), with increasing the helix angle, the length of two - pair engagement increases and the length of one-pair engagement (central phase) decreases. Also, the length of the right phase of two-pair engagement increases. At $\beta = 0°$, the pressure $p_{j\max}$ at the teeth' entrance to the left phase of two-pair engagement will be slightly lower (by 1.09 times) than at the teeth' entrance to the one-pair engagement. At the helix angle $\beta = 5°$, the highest $p_{j\max}$ are close at these points of engagement of teeth and are 1.07 times lower than at $\beta = 0°$. Accordingly, at $\beta = 5°$, the total overlap ratio is $\varepsilon_\gamma = \varepsilon_\alpha + \varepsilon_\beta = 1.741$ compared with the end overlap ratio ε_α = 1.372 at $\beta = 0°$.

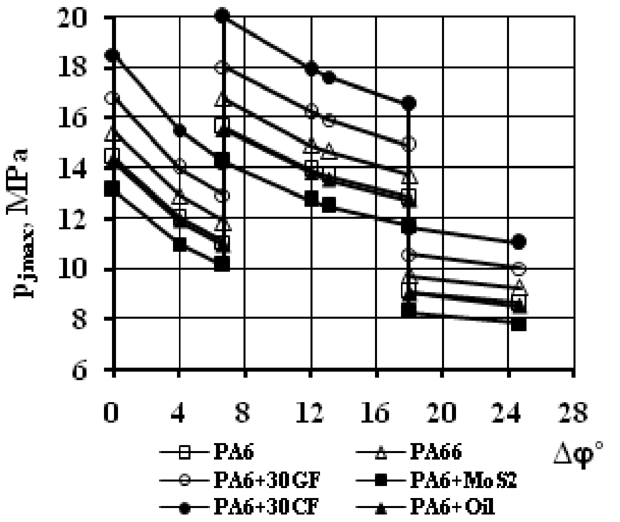

(a)

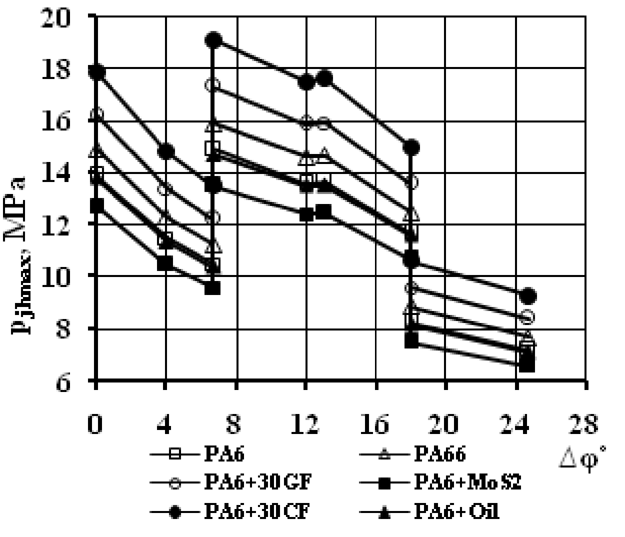

(b)

Fig. 2. Maximum contact pressures in the meshing at β = 0°: a) before wear, b) after wear of the wheel teeth.

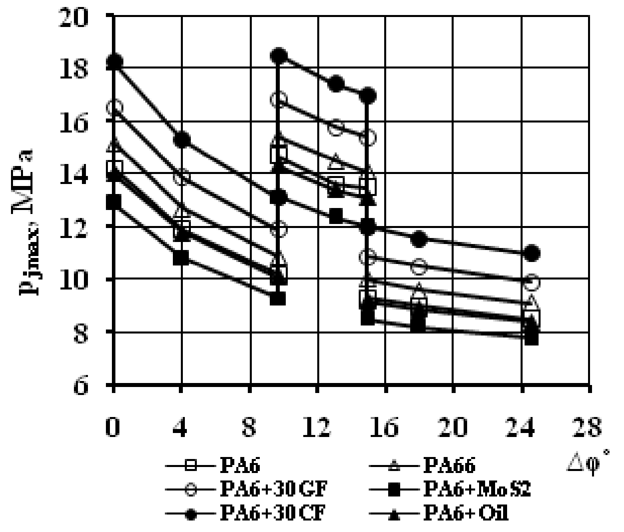

(a)

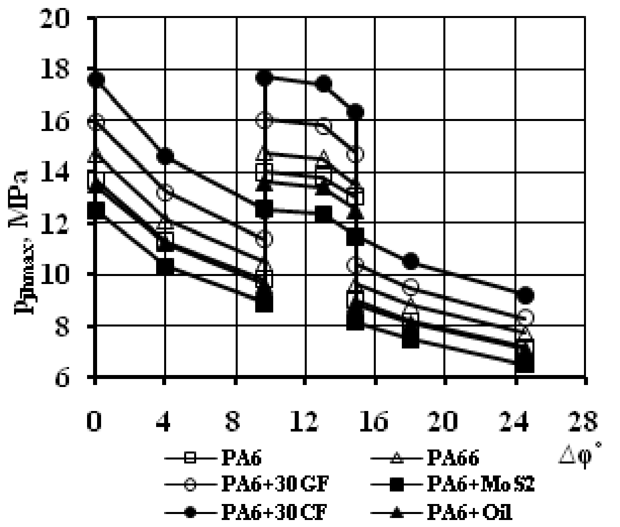

(b)

Fig. 3. Maximum contact pressures in the meshing at β = 5°: a) before wear, b) after wear of the wheel teeth.

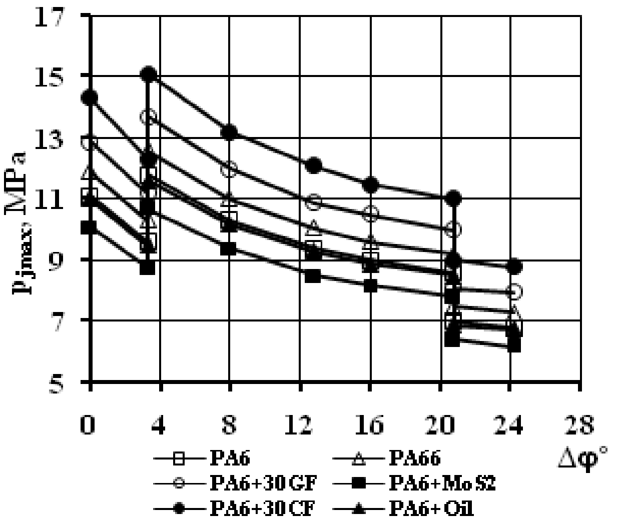

(a)

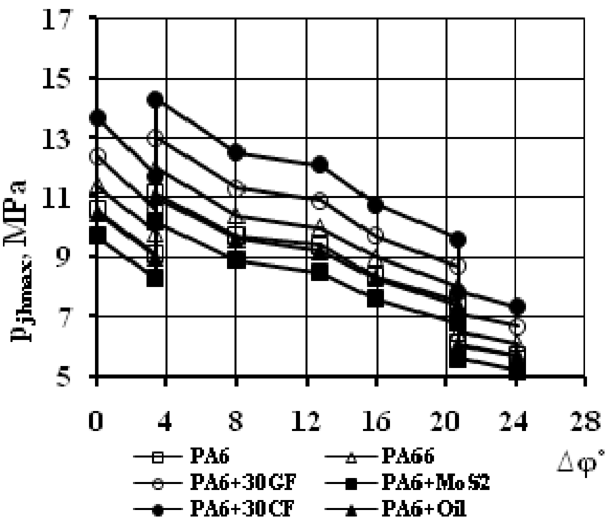

(b)

Fig. 4. Maximum contact pressures in the meshing at β = 10°: a) before wear, b) after wear of the wheel teeth.

At a helix angle of $\beta = 10^0$ there is observed a three-two-three-pair engagement with an overlap ratio of ε_γ = 2.033. Accordingly, the left and right areas of the three-pair engagement are narrow, while the central area of the two-pair engagement is large. The maximum contact pressures at the teeth' entrance to the left phase of the three-pair engagement is 1.07 times lower than that at the teeth' entrance to the two-pair engagement. On the other hand, the reduction in $p_{j\max}$ in helical gears is up to by 1.33 times compared to the spur gears.

The research results demonstrate that the use of MoS_2 and oil fillers for the basic polyamide PA6 allows one to slightly lower the maximum contact pressures $p_{j\max}$ in the engagement. When using 30% GF and 30% CF as fillers, the maximum contact pressures increase significantly. In particular, the ratio of maximum contact pressures in gears with a gear made of PA6+30CF relative to ones for unfilled polyamide PA6 is 1.28. In general, the pressure variation reaches 1.41 times (PA6+30CF relative to PA6+MoS_2). Undoubtedly, this fact will also affect the durability of gears, which will be shown below.

The important role of the composition of PA6-based composites in the change of contact pressures $p_{j\max}$ confirms the decisive influence of Young's modulus on $p_{j\max}$. The higher Young's modulus of the polymer material relative to PA6, the higher the contact pressures. Correspondingly, the pressures will be lower for smaller Young's moduli.

The wear of polymer gear teeth leads to a decrease in the pressure $p_{j\max}$ at the entrance to the two-pair (three-pair) and one-pair (two-pair) engagement by ≈ 1.055 times, regardless of the helix angle, as shown in Figures 2b, 3b, and 4b. The tooth wear has a significantly greater impact on reduction in $p_{j\max}$ at the exit from one-pair engagement and in the right phase of two-pair engagement (up to by 1.2 times).

On the other hand, the operation conditions of MP gears are significantly improved in helical gears compared to spur gears. It is because they have a much larger engagement area with a higher parity of the teeth contact, even at an angle of $\beta =$ 5° (Fig. 3a). At a helix angle of 10° (Fig. 4a) with three-two-three-pair engagement, the area of three-pair engagement is smaller than that of two-pair one.

The trend of the linear wear h_{2j} of polymer gear teeth at selected points of engagement depending on different helix angles is shown in Fig. 5.

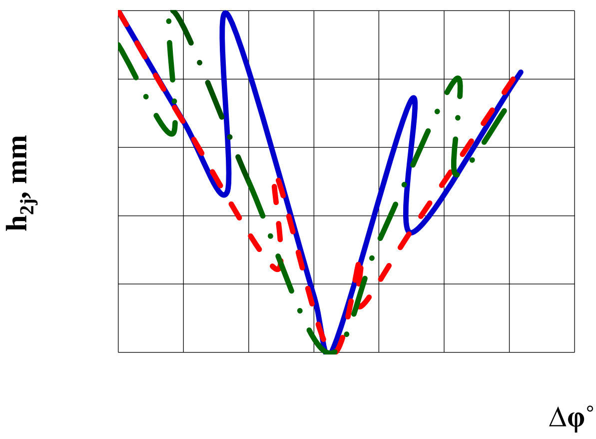

Fig. 5. Linear wear of polymer gear tooth profile during engagement: solid line for β = 0°, dashed line for β = 5°, and dash-dotted line for β = 10°.

In a spur gear, where β = 0, the acceptable wear h_{2*} = 0.5 mm of the gear teeth is reached at their entrance to the left phase of the two-pair engagement. At the entrance to the one-pair engagement, the tooth wear is close to the acceptable one. That is, at these two characteristic points of engagement, tooth wear is almost equal. At the exit of the teeth from the one-pair and the second phase of two-pair engagement, the wear is smaller.

In helical gears with the helix angle β = 5°, the distribution of their wear will be somewhat different. The acceptable tooth wear will also be achieved at the entrance to the left phase of the two-pair engagement. At the entrance to the one-pair engagement (central zone) it will be significantly lower than that in spur gears. At the exit of teeth from the second phase of two-pair engagement, their wears will be close.

At the helix angle β = 10° (three-two-three-pair engagement), the acceptable wear of teeth is achieved at the entrance to the two-pair engagement (central zone). At the exit of the teeth from the central and final phases of engagement, their wear will be close.

For all studied polyamides, patterns of the tooth linear wear presented in Fig. 5 are the same during the engagement phase.

On the contrary, the estimated minimum durability $t_{B\min}$ of gears made of different types of polyamides will be significantly different depending on the helix angle (Fig. 6).

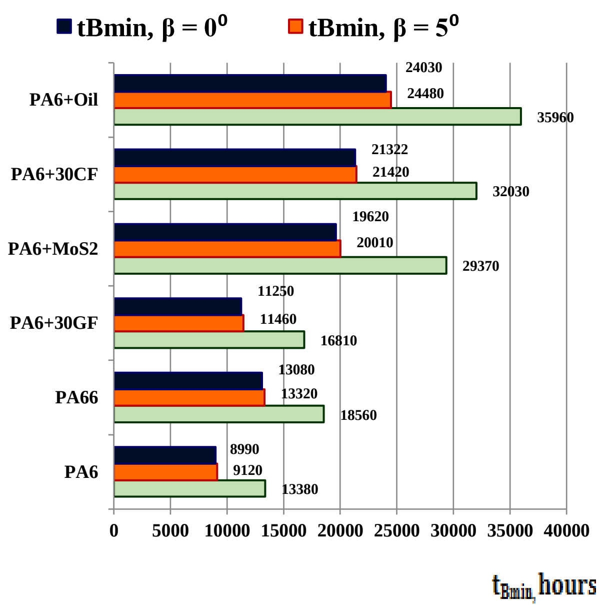

Fig. 6. Minimum durability of MP gears at different helix angles with the acceptable wear of gear teeth.

Minimum gear durability is the durability at the point of the tooth profile where the acceptable wear is reached (Fig. 5). It, as noted above, will occur at different points for different helix angles.

The lowest durability will be for gears made of unfilled polyamide PA6. The durability of gears made of PA6+30GF will be 1.25 times higher than that of PA6. The durability ratio of gears made of PA66 and PA6 is 1.46. The gears made of polyamide composites have significantly higher durability: PA6+MoS_2 by 2.19 times, PA6+30CF by 2.43 times), and PA6+Oil by 2.68 times.

Fig. 7 presents a relative evaluation of MP gears durability depending on the helix angle for gear made of different polymeric materials.

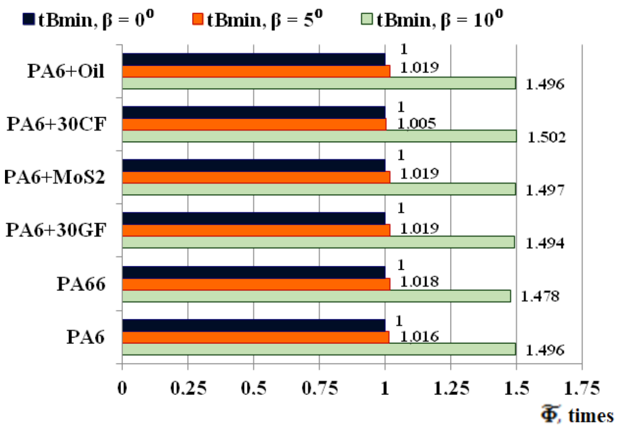

Fig. 7. The relative durability of MP gears at different helix angles.

In helical gears with a helix angle of β = 5°, a slight increase in durability is achieved as compared to spur gears (up to by 1.019 times). This can be related to the slight decrease in the contact pressures $p_{0\max}$ at the tooth entrance to the two-pair engagement at the angle β = 5° compared to β = 0 (point j = 0, where the acceptable h_{2*} = 0.5 mm is reached) (Fig. 5, Tables A1 and A2 in Appendices). For example, in gears made of PA6, $p_{0\max}$ = 14.2 MPa (β = 5°), $p_{0\max}$ = 14.4 MPa (β = 0). Also, at a helix angle of β = 5°, the total contact ratio $\varepsilon_\gamma = \varepsilon_\alpha + \varepsilon_\beta = 1.741$. It leads to a significant narrowing of the one-pair engagement phase (Fig. 2). At β = 0, the end overlap ratio ε_α equals 1.372. At the helix angle β = 10°, the durability of MP gears for all polymer materials studied increases by about 1.5 times due to the 1.225-fold decrease in contact pressure $p_{2\max}$ in point j = 2, where h_{2*} = 0.5 mm is reached for three-two-three-pair engagement (Fig. 5, Table A3).

In the Appendix, the tables show the results of the calculations based on which the diagrams were built and analyzed.

4. CONCLUSIONS

The basic qualitative regularities of the effect of tooth wear and engagement parity on maximum contact pressures, linear teeth wear along the profile, and resource of MP helical gears at different helix angles have been established.

1. The highest contact pressures occur in engagement when using PA6+30CF, and they are slightly lower for PA6+30GF. The level of pressure depends on Young's modulus, and it is the highest in these composites (Table 1). The lowest maximum pressures are characteristic for the composite PA6 + MoS_2.
2. n spur gears, the linear wear of teeth is differentiated during their engagement. The point of engagement where the acceptable tooth wear is reached is located at the entrance to the left phase of the two-one-two-pair engagement. In helical gears, it is either at the entrance to the left phase of the two-one-two-pair engagement, or at the entrance to the central phase of the three-two-three-pair engagement.
3. At the helix angle β = 10°, the gear durability increases significantly due to the occurrence of the three-two-three-pair engagement and the maximum contact pressure in the engagement decreases. The gears with PA6 polyamide gear have the lowest durability. The durability of MP gears with a gear made of polyamide composites PA6+MoS_2, PA6+30CF, and PA6+Oil will be much higher. Filling of the base polyamide PA6 with different components makes it possible to increase the durability of MP gears by 2.68 times.

4. Important for engineering practice issues of assessing the teeth' contact strength at the most loaded contact points and predicting the gears' durability, as well as a very important task of optimal choice of polymer materials for MP gears according to these criteria have been effectively solved thanks to using the newly developed generalized (complex) analytical method. The method expands the possibilities of MP gears research in comparison with the calculation methods for metal gears given in the standards ISO 6336 - 2 [29], DIN 3900 [30], and VDI 2736 [31]. In particular, using the method at any point of teeth engagement makes it possible to assess the maximum contact pressure, sliding speed, radius of curvature of the tooth profile, linear wear of teeth, gear durability; to determine the angles of change in the engagement type (two-one-two-pair or three-two-three-pair), and the angle of the tooth exit from the engagement; to consider the influence of tooth wear on the change in the curvature radius of the profile, on contact pressures, and gear durability, and to consider the effect of gears correction (was not investigated in this article) on the contact and tribological characteristics of MP gears.

REFERENCES

[1] S.V. Shilko and V.E. Starzhinsky, "Calculation of wear resistance of gear transmission with wheels from reinforced composite materials," *Friction and Wear*, vol. 13, no. 3, pp. 444–451, 1993.

[2] Yu.N. Drozdov, "On the development of methods for calculating wear and friction modeling," *Wear resistance*, pp. 120–135, 1975.

[3] C. J. Hooke, S. N. Kukureka, P. Liao, M. Rao, and Y. K. Chen, "The friction and wear of polymers in non-conformal contacts," *Wear*, vol. 200, no. 1–2, pp. 83–94, Dec. 1996, doi: 10.1016/s0043-1648(96)07270-5.

[4] G. Kalacska, M. Kozma, P. De Baets, R. Keres ztes, L. Zsidai, "Friction and Wear of Engine ering Polymer Gears", *in World Tribology Congress III, Washington, USA*, 12–16 September 2005, pp. 259–260, doi: 10.1115/WTC2005-63961.

[5] R. Keresztes, G. Kalacska, "Friction of Polyme r/Steel Gear Pairs," *Plastics and Rubber*, vol. 45, pp. 236-242, 2008.

[6] J. Sukumaran *et al.*, "Modelling gear contact with twin-disc setup," *Tribology International*, vol. 49, pp. 1–7, May 2012, doi: 10.1016/j.triboint.2011.12.007.

[7] JJ. Cathelin, E. Letzelter, M. Guingand, J. P. De Vaujany, and L. Chazeau, "Experimental and numerical study of a loaded cylindrical PA66 gear," *Journal of Mechanical Design*, vol. 135, no. 4, Mar. 2013, doi: 10.1115/1.4023634.

[8] S. Yousef, T. Osman, M. F. Khattab, A. A. Bahr, and A. M. Youssef, "A new design of the Universal Test rig to measure the wear characterizations of polymer acetal gears (Spur, helical, bevel, and worm)," *Advances in Tribology*, vol. 2015, pp. 1–8, Jan. 2015, doi: 10.1155/2015/926918.

[9] A. G. De Almeida Rosa, J. A. Moreto, M. D. Manfrinato, and L. S. Rossino, "Study on friction and wear behavior of SAE 1045 steel, reinforced nylon 6.6 and NBR rubber used in clutch disks," *Materials Research*, vol. 17, no. 6, pp. 1397–1403, Dec. 2014, doi: 10.1590/1516-1439.282714.

[10] M.V. Kulkarni, K. Elangovan, K.R. Hemachandra, S.J. Basappa, "Tribological behaviours of ABS and PA6 polymer metal sliding combinations under dry friction, water absorbed and electroplated conditions", *Journal of Engineering Science and Technology*, vol. vol. 11, no. 1, pp. 068-084, Jan. 2016.

[11] AA. Pogačnik, A. Kupec, and M. Kalin, "Tribological properties of polyamide (PA6) in self-mated contacts and against steel as a stationary and moving body," *Wear*, vol. 378–379, pp. 17–26, May 2017, doi: 10.1016/j.wear.2017.01.118.

[12] J. Jóźwik, K. Dziedzic, M. Barszcz, and M. I. Pashechko, "Analysis and comparative assessment of basic tribological properties of selected polymer composites," *Materials*, vol. 13, no. 1, p. 75, Dec. 2019, doi; 10.3390/ma13010075.

[13] M. Kurokawa, Y. Uchiyama, T. Iwai, and S. Nagai, "Performance of plastic gear made of carbon fiber reinforced polyamide 12," *Wear*, vol. 254, no. 5–6, pp. 468–473, Mar. 2003, doi: 10.1016/S0043-1648(03)00020-6.

[14] J. Tavčar, G. Grkman, and J. Duhovnik, "Accelerated lifetime testing of reinforced polymer gears," *Journal of Advanced Mechanical Design, Systems and Manufacturing*, vol. 12, no. 1, p. JAMDSM0006, Jan. 2018, doi: 10.1299/jamdsm.2018jamdsm0006.

[15] K. Mao, W. Li, C. J. Hooke, and D. Walton, "Friction and wear behaviour of acetal and nylon gears," *Wear*, vol. 267, no. 1–4, pp. 639–645, Jun. 2009, doi: 10.1016/j.wear.2008.10.005.

[16] K. Mao, "A new approach for polymer composite gear design," *Wear*, vol. 262, no. 3–4, pp. 432–441, Feb. 2007, doi 10.1016/j.wear.2006.06.005.

[17] S. Singh, Y. K. Yadav, Siddhartha, and A. Chandra, "Exploration on Wear Characteristics: Performance of gears of polyamide66," in *Lecture notes in mechanical engineering*, 2020, pp. 581–589. doi: 10.1007/978-981-15-8704-7_71.

[18] K. Harsha and Y. S. Rao, "Experimental Investigation on wear behaviour of Polymer based Spur Gears – A Review," *Zenodo (CERN European Organization for Nuclear Research)*, Mar. 2020, doi: 10.5281/zenodo.3698538.

[19] H. Nigus, "Review: Failure Detection Method of Polymer Composite Gears," *HAL (Le Centre Pour La Communication Scientifique Directe)*, Aug. 2017, doi: 10.2412/mmse.54.24.7.

[20] M. V. Chernets, С. В. Шилько, M. I. Pashechko, and M. Barshch, "Wear resistance of glass- and Carbon-Filled polyamide composites for Metal-Polymer gears," *Journal of Friction and Wear*, vol. 39, no. 5, pp. 361–364, Sep. 2018, doi: 10.3103/S1068366618050069.

[21] M. V. Chernets, "Method of calculation of tribotechnical characteristics of the metal-polymer gear, reinforced with glass fiber, taking into account the correction of tooth," *Eksploatacja I Niezawodność*, vol. 21, no. 4, pp. 546–552, Dec. 2019, doi: 10.17531/ein.2019.4.2.

[22] M. V. Chernets and A. Kornienko, "Prediction of the service life of Metal-Polymer gears made of glass and carbon Fibre-Reinforced polyamide, considering the impact of height correction," *Advances in Sciences and Technology/Postępy Nauki I Techniki*, vol. 14, no. 3, pp. 15–21, Sep. 2020, doi: 10.12913/22998624/124553.

[23] M. V. Chernets, A. Kornienko, Y. Chernets, and C. Федорчук, "Modelling of contact and tribotechnical parameters of metal–polymer gears taking into account wear and correction of teeth," *Proceedings of the Institution of Mechanical Engineers. Part J, Journal of Engineering Tribology*, vol. 236, no. 7, pp. 1263–1272, Nov. 2021, doi: 10.1177/13506501211054683.

[24] M. V. Chernets, M. Opielak, and A. Kornienko, "Comparison of Load-Carrying Capacity, Wear, and Resource of Metal-Polymer Corrected Spur Gears with a Gear Made of Polyamides PA6 or PA6+30CF," *StrojnišKi Vestnik*, vol. 68, no. 11, pp. 713–721, Nov. 2022, doi: 10.5545/sv-jme.2022.242.

[25] M. V. Chernets, R. Ya. Yarema, and Yu. M. Chernets, "A method for the evaluation of the influence of correction and wear of the teeth of a cylindrical gear on its durability and strength. Part 1. Service life and wear," *Materials Science*, vol. 48, no. 3, pp. 289–300, Nov. 2012, doi: 10.1007/s11003-012-9505-y.

[26] M. V. Chernets and Ju. M. Chernets, "Evaluation of the strength, wear, and durability of a corrected cylindrical involute gearing, with due regard for the tooth engagement conditions," *Journal of Friction and Wear*, vol. 37, no. 1, pp. 71–77, Jan. 2016, doi: 10.3103/S1068366616010050

[27] M. V. Chernets and Yu. M. Chernets, "A technique for calculating tribotechnical characteristics of tractive cylindrical gear of VL-10 locomotive," *Journal of Friction and Wear*, vol. 38, no. 1, pp. 23–29, Jan. 2017, doi: 10.3103/S1068366616060040.

[28] M. V. Chernets and J. Chernets, "The simulation of influence of engagement conditions and technological teeth correction on contact strength, wear and durability of cylindrical spur gear of electric locomotive," *Proceedings of the Institution of Mechanical Engineers. Part J, Journal of Engineering Tribology*, vol. 231, no. 1, pp. 57–62, Aug. 2016, doi: 10.1177/1350650116645024.

[29] *Calculation of load capacity of spur and helical gears*, ISO 6336:2006-10, 2006.

[30] *Trägfähigkeitsberechnung von Stirnrädern, Einführung und allgemeine Einflussfaktoren*, DIN 3990:1987-12, 1987.

[31] *Thermoplastische Zahnräder – Stirnradgetriebe –Tragfähigkeits-berechnung*, VDI 2736 Blatt 2:2014-06, 2014.

NOMENCLATURE

a	center distance of gear pair, mm
B	calculation block size, rev
b	width of pinion, mm
$2b_j$	width of contact area, mm
C_k, m_k	wear resistance characteristics of gear materials, [-]

E	Young's modulus of gear tooth materials, MPa
f	sliding friction coefficient, [-]
h_{k*}	acceptable wear of composite gear, mm
h'_{kj}	single linear wear of gear teeth at any j-th point of tooth profile, mm
h_{kjn}	total wear of gear teeth, mm
h_{kjB}	wear of gear teeth in individual interaction block, mm
i =1, 2, …	load levels, [-]
j	contact points on the active face of the teeth, [-]
j = 0, j = s	the first and the last point of tooth engagement, respectively, [-]
K_g	dynamic factor, [-]
k = 1; 2	number of gears (1 – pinion, 2 – gear)
m	engagement module, mm
N	force acting in tooth engagement, N
n_1	number of pinion revolutions, rpm
P	power on drive shaft (pinion), kW
p_b	pitch of teeth, mm
$p_{j\,\max}$	maximum contact pressure at the j-th point of contact, MPa
$p_{jh\,\max}$	maximum tribocontact pressure (for tooth wear) at the j-th point of contact, MPa
R_m	immediate tensile strength of material, MPa
r	radius of gear tooth fillet, mm
r_1, r_2	pitch circle radii of pinion and gear, respectively, mm
r_{b1}, r_{b2}	base circle radii of pinion and gear, respectively, mm
r_{a1}, r_{a2}	addendum circle radii of pinion and gear,respectively, mm
l_{min}	minimum contact line length, mm
T_{nom}	rated torque, Nmm
t'_j	time of contact at displacement of the j-th point of contact along tooth profile by contact area width $2b_j = const,$ sec
$t_{B\,\min}$	minimal durability as calculated by the block method, h
u	gear ratio, [-]
$v_j=v$	sliding speed at the j-th point of tooth profile, m/sec
v_0	velocity of the contact point along tooth profile, m/sec
w	number of engaged tooth pairs, [-]
z_1, z_2	numbers of pinion teeth and gear teeth, respectively, [-]

Greek letters

α	pressure angle of engaged teeth, °
α_t	end pressure angle, °
α_{t10}	angle of the first point on contact line,
α_{t1s}	angle describing location of the last point of engagement of pinion teeth on contact line, °
α_{t20}, α_{t2s}	angles describing location of the first and last points of engagement of gear teeth on contact line, °
β	helix angle, °
$\Delta\varphi$	selected angle of rotation of pinion teeth from the point of initial contact (point 0) to point 1, and so on, °
μ	Poisson's ratio of gear tooth materials, [-]
ω_1	angular velocity of pinion, sec^{-1}
ρ_j	reduced curvature radius of gear profile due to wear, in a normal section, mm
ρ_{1j}, ρ_{2j}	initial curvature radii of the profiles of pinion teeth and gear teeth, respectively, mm
ρ_{jh}	reduced curvature radius of the gear profile due to wear, mm
ρ_{1jh}, ρ_{2jh}	variable curvature radii of the profiles of pinion teeth and gear teeth, respectively, mm
τ_S	shear strength of material, MPa
$\tau_{j\max}$	maximum specific friction force according to Coulomb's law, MPa
ε_α,ε_β	gear end and pitch overlap ratios, respectively, [-]
n_α,n_β	fractional parts of end and pitch overlap ratios, respectively, [-]

Appendices

Table A1

$\beta = 0$ Polymers	Parameters									
		j =0	*j* = 1	*j* = 2	*j* = 2	*j* = 3	*j* = 4	*j* = 5	*j* = 5	*j* = 6
PA6	$p_{j\max}$, MPa	14.4	12	11.05	15.6	13.9	13.65	12.8	9.05	8.6
	$p_{jh\max}$, MPa	13.9	11.5	10.5	14.9	13.6	13.65	11.7	8.26	7.2
	h_{2j}, mm	0.5	0.338	0.235	0.495	0.083	0	0.37	0.175	0.41
	$t_{B\min}$, hours	8990								
	$\Delta\varphi$,°	0	4	6.69	6.69	12	13.08	18	18	24.7
PA66	$p_{j\max}$, MPa	15.4	12.9	11.84	16.74	14.9	14.64	13.7	9.7	9.2
	$p_{jh\max}$, MPa	14.9	12.3	11.28	15.9	14.6	14.64	12.5	8.86	7.7
	h_{2j}, mm	0.5	0.338	0.235	0.495	0.083	0	0.37	0.175	0.41
	$t_{B\min}$, hours	13080								
PA6+30GF	$p_{j\max}$, MPa	16.8	14	12.9	18.2	16.2	15.9	14.9	10.55	10
	$p_{jh\max}$, MPa	16.2	13.4	12.2	17.31	15.85	15.9	13.6	9.6	8.4
	h_{2j}, mm	0.5	0.338	0.235	0.495	0.083	0	0.37	0.175	0.41
	$t_{B\min}$, hours	11250								
PA6+MoS_2	$p_{j\max}$, MPa	13.1	10.96	10.1	14.25	12.7	12.45	11.7	8.25	7.8
	$p_{jh\max}$, MPa	12.7	10.46	9.6	13.5	12.4	12.45	10.7	7.5	6.6
	h_{2j}, mm	0.5	0.338	0.235	0.495	0.083	0	0.37	0.175	0.41
	$t_{B\min}$, hours	19620								
PA6+30CF	$p_{j\max}$, MPa	18.5	15.5	14.2	20.1	17.9	17.6	16.5	11.6	11
	$p_{jh\max}$, MPa	17.9	14.8	13.5	19.1	17.5	17.6	15	10.6	9.3
	h_{2j}, mm	0.5	0.338	0.235	0.495	0.083	0	0.37	0.175	0.41
	$t_{B\min}$, hours	21532								
PA6+Oil	$p_{j\max}$, MPa	14.25	11.9	10.9	15.5	13.8	13.5	12.7	9	8.5
	$p_{jh\max}$, MPa	13.8	11.35	10.4	14.7	13.5	13.5	11.6	8.2	7.1
	h_{2j}, mm	0.5	0.338	0.235	0.495	0.083	0	0.37	0.175	0.41
	$t_{B\min}$, hours	24030								

Table A2

$\beta = 5^{\circ}$	Parameters									
Polymers		*j* =0	*j* = 1	*j* = 2	*j* = 2	*j* = 3	*j* = 4	*j* = 5	*j* = 5	*j* = 6
PA6	$p_{j\max}$, MPa	14.2	11.9	10.2	14.7	13.6	13.5	9.3	9	8.5
	$p_{jh\max}$, MPa	13.7	11.3	9.8	14.4	13.6	13.2	9.0	8.2	7.15
	h_{2j}, mm	0.5	0.337	0.122	0.26	0	0.14	0.067	0.179	0.412
	$t_{B\min}$, hours	9120								
	$\Delta\varphi$,°	0	4	9.67	9.67	13.01	14.87	14.87	18	24.57
PA66	$p_{j\max}$, MPa	15.2	12.7	10.9	15.4	14.5	14.1	10	9.6	9.1
	$p_{jh\max}$, MPa	14.7	12.1	10.45	14.75	14.5	13.5	9.6	8.8	7.7
	h_{2j}, mm	0.5	0.337	0.122	0.26	0	0.14	0.067	0.179	0.412
	$t_{B\min}$, hours	13320								
PA6+30GF	$p_{j\max}$, MPa	16.5	13.85	11.9	16.8	15.8	15.4	10.9	10.5	9.9
	$p_{jh\max}$, MPa	15.95	13.2	11.35	16.05	15.8	14.7	10.4	9.5	8.3

	h_{2j}, mm	0.5	0.337	0.122	0.26	0	0.14	0.067	0.179	0.412
	$t_{B\min}$, hours	11460								
PA6+MoS2	$p_{j\max}$, MPa	12.9	10.8	9.3	13.15	12.35	12	8.5	8.2	7.8
	$p_{jh\max}$, MPa	12.5	10.3	8.9	12.55	12.35	11.5	8.15	7.5	6.5
	h_{2j}, mm	0.5	0.337	0.122	0.26	0	0.14	0.067	0.179	0.412
	$t_{B\min}$, hours	20010								
PA6+30CF	$p_{j\max}$, MPa	18.25	15.3	13.1	18.5	17.4	17	12	11.55	11
	$p_{jh\max}$, MPa	17.6	14.6	12.5	17.7	17.4	16.3	11.5	10.5	9.2
	h_{2j}, mm	0.5	0.337	0.122	0.26	0	0.14	0.067	0.179	0.412
	$t_{B\min}$, hours	21420								
PA6+Oil	$p_{j\max}$, MPa	14	11.8	10.1	14.3	13.4	13.1	9.2	8.9	8.4
	$p_{jh\max}$, MPa	13.5	11.2	9.6	13.6	13.4	12.5	8.85	8.1	7.1
	h_{2j}, mm	0.5	0.337	0.122	0.26	0	0.14	0.067	0.179	0.412
	$t_{B\min}$, hours	24480								

Table A3

$\beta = 10^{\circ}$ Polymers	Parameters									
		j =0	j = 1	j = 2	j = 2	j = 3	j = 4	j = 5	j = 5	j = 6
PA6	$p_{j\max}$, MPa	11.1	9.6	11.8	10.3	9.4	9	8.6	7	6.8
	$p_{jh\max}$, MPa	10.6	9.1	11.15	9.7	9.4	8.35	7.5	6.1	5.7
	h_{2j}, mm	0.45	0.32	0.5	0.25	0	0.163	0.4	0.26	0.37
	$t_{B\min}$, hours			13380						
	$\Delta\varphi$,°	0	3.35	3.35	8	12.78	16	20.73	20.73	24.165
PA66	$p_{j\max}$, MPa	11.9	10.3	12.6	11	10.05	9.6	9.2	7.5	7.3
	$p_{jh\max}$, MPa	11.4	9.8	12	10.4	10	9	8	6.5	6.1
	h_{2j}, mm	0.45	0.32	0.5	0.25	0	0.163	0.4	0.26	0.37
	$t_{B\min}$, hours			18470						
PA6+30GF	$p_{j\max}$, MPa	12.9	11.2	13.7	12	10.9	10.5	10	8.1	7.95
	$p_{jh\max}$, MPa	12.4	10.6	13	11.3	10.9	9.7	8.7	7.1	6.7
	h_{2j}, mm	0.45	0.32	0.5	0.25	0	0.163	0.4	0.26	0.37
	$t_{B\min}$, hours			16810						
PA6+MoS2	$p_{j\max}$, MPa	10.1	8.75	10.7	9.4	8.5	8.2	7.8	6.4	6.2
	$p_{jh\max}$, MPa	9.7	8.3	10.2	8.9	8.5	7.6	6.8	5.6	5.2
	h_{2j}, mm	0.45	0.32	0.5	0.25	0	0.163	0.4	0.26	0.37
	$t_{B\min}$, hours			29370						
PA6+30CF	$p_{j\max}$, MPa	14.3	12.3	15.1	13.2	12.1	11.5	11	9	8.8
	$p_{jh\max}$, MPa	13.7	11.7	14.3	12.5	12.1	10.75	9.6	7.85	7.35
	h_{2j}, mm	0.45	0.32	0.5	0.25	0	0.163	0.4	0.26	0.37
	$t_{B\min}$, hours			32030						
PA6+Oil	$p_{j\max}$, MPa	11	9.5	11.6	10.2	9.3	8.9	8.5	6.9	6.75
	$p_{jh\max}$, MPa	10.5	9	11	9.6	9.2	8.3	7.4	6.05	5.7
	h_{2j}, mm	0.45	0.32	0.5	0.25	0	0.163	0.4	0.26	0.37
	$t_{B\min}$, hours			35960						